Analytical Derivation of Cosserat Moduli via Homogenization of Heterogeneous Elastic Materials

D. Bigoni[1]
Dipartimento di Ingegneria Meccanica e Strutturale,
Università di Trento,
Via Mesiano 77,
38050 Povo, Trento, Italy
e-mail: bigoni@ing.unitn.it

W. J. Drugan
Dipartimento di Ingegneria Meccanica e Strutturale,
Università di Trento,
Via Mesiano 77,
38050 Povo, Trento, Italy
and
Department of Engineering Physics,
University of Wisconsin-Madison,
1500 Engineering Drive,
Madison, WI 53706-1687
e-mail: drugan@engr.wisc.edu

Why do experiments detect Cosserat-elastic effects for porous, but not for stiff-particle-reinforced, materials? Does homogenization of a heterogeneous Cauchy-elastic material lead to micropolar (Cosserat) effects, and if so, is this true for every type of heterogeneity? Can homogenization determine micropolar elastic constants? If so, is the homogeneous (effective) Cosserat material determined in this way a more accurate representation of composite material response than the usual effective Cauchy material? Direct answers to these questions are provided in this paper for both two- (2D) and three-dimensional (3D) deformations, wherein we derive closed-form formulae for Cosserat moduli via homogenization of a dilute suspension of elastic spherical inclusions in 3D (and circular cylindrical inclusions in 2D) embedded in an isotropic elastic matrix. It is shown that the characteristic length for a homogeneous Cosserat material that best mimics the heterogeneous Cauchy material can be derived (resulting in surprisingly simple formulae) when the inclusions are less stiff than the matrix, but when these are equal to or stiffer than the matrix, Cosserat effects are shown to be excluded. These analytical results explain published experimental findings, correct, resolve and extend prior contradictory theoretical (mainly numerical and limited to two-dimensional deformations) investigations, and provide both a general methodology and specific results for determination of simple higher-order homogeneous effective materials that more accurately represent heterogeneous material response under general loading conditions. In particular, it is shown that no standard (Cauchy) homogenized material can accurately represent the response of a heterogeneous material subjected to a uniform plus linearly varying applied traction, while a homogenized Cosserat material can *do so (when inclusions are less stiff than the matrix).* [DOI: 10.1115/1.2711225]

Keywords: homogenization, Cosserat-elasticity, dilute suspension of elastic spheres, nonlocal constitutive equations, micropolar effects

1 Introduction

There is a long-standing debate in the solid mechanics community concerning the possibility of predicting micropolar elastic (Cosserat) behavior from Cauchy-elastic materials containing inhomogeneities or microstructures. In fact, although the motivation leading to Cosserat effects seems to be very intuitive, theoretical results in the literature are often contradictory and no definitive conclusion is available (see Appendix A for details). Moreover, experimental results support Cosserat effects for porous materials (like bone or foam [1–5]), but find an absence of these effects for reinforced materials [6,7].

In the present paper we provide a general methodology for the determination of the moduli for a homogeneous Cosserat-elastic material that best approximates a heterogeneous Cauchy-elastic material. We apply this methodology to the specific cases of three-dimensional (3D) deformations of a dilute suspension of (Cauchy, linear, and isotropic) elastic spherical inclusions, and two-dimensional (2D) deformations of circular cylindrical inclusions, in a (Cauchy, linear, and isotropic) elastic matrix. With reference to a Cosserat (linear and isotropic) material, it is shown that:

1. Cosserat effects are predicted for spherical or cylindrical inclusions less stiff than the matrix, but are excluded for inclusions having stiffness equal to or greater than that of the matrix;
2. simple, closed-form formulae give the Cosserat characteristic length (and the other effective Cosserat moduli) as a function of the inclusion radius, volume fraction, and the elastic contrast of the constituent phases; and
3. the characteristic length that results for three-dimensional deformations of a matrix with spherical inclusions is significantly smaller than that resulting for two-dimensional deformations of a matrix with circular cylindrical inclusions.

Conclusion (1) rigorously explains experimental evidence demonstrating micropolar effects for porous material, but displaying an opposite trend, or in the words of Gauthier [7] "an anti-micropolar phenomenon," for inclusions stiffer than the matrix.

A closely related issue is that standard homogenization results for linear elastic materials provide overall or effective elastic moduli that relate (*uniform*) average stress to (*uniform*) average strain. This means that standard homogenization results give a homogeneous "effective" material that is able to represent well the overall response of the actual heterogeneous elastic material *when the applied loading is uniform*. However, when the applied loading deviates from uniformity, the homogeneous "effective" material less accurately represents the overall response of the actual heterogeneous material. This fact is important, since of course in general composite materials are employed in applications where the applied loading is not uniform.

We show in this paper, for situations in which the applied loading on a heterogeneous material varies sufficiently slowly that it admits a Taylor series expansion, that whereas the standard homogenization results provide a homogeneous "effective" material that can accurately represent the actual heterogeneous one only

[1]Corresponding author.

Contributed by the Applied Mechanics Division of ASME for publication in the JOURNAL OF APPLIED MECHANICS. Manuscript received February 10, 2006; final manuscript received April 20, 2006. Review conducted by Robert M. McMeeking.

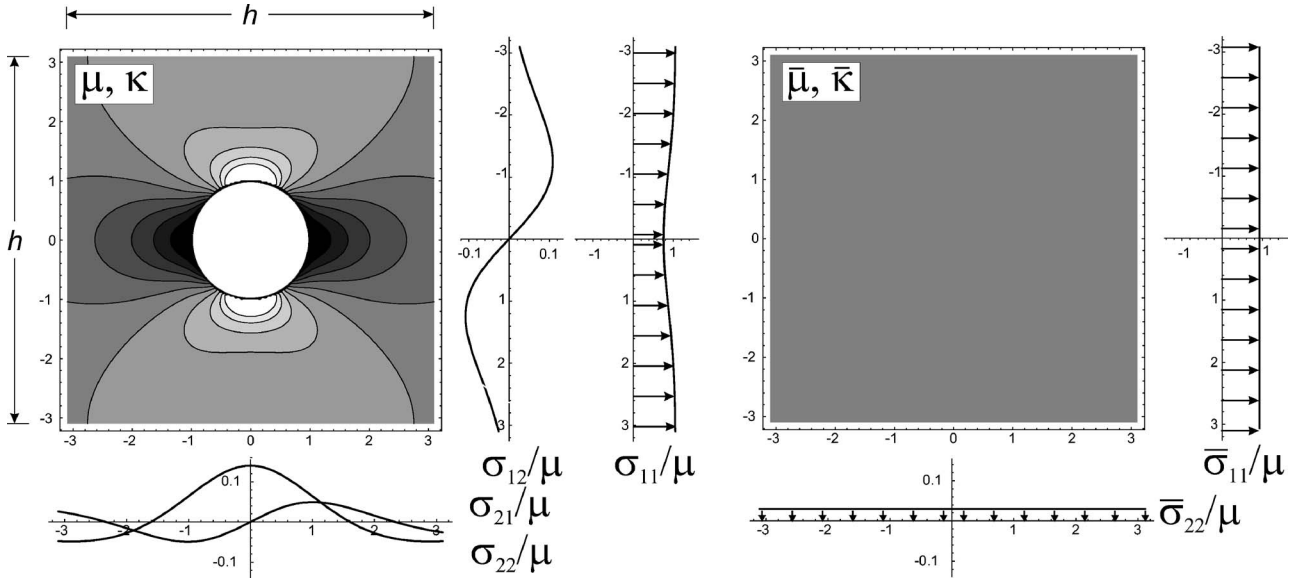

Fig. 1 Procedure of homogenization of a material containing a dilute distribution of circular voids. Heterogeneous material (left) is an $h\times h$ prism removed from an infinite sheet that is subjected to uniform, uniaxial far-field stress; homogeneous material (right) is subjected to the mean stresses calculated from the heterogeneous prism. For the plane strain problem, level sets of σ_{11} are shown; note that the values of σ_{12}, σ_{21}, and σ_{22}, shown parallel to the edges, are less than 1/10 the maximum value of σ_{11} at a distance from inclusion center equal to three times the radius of the inclusion.

when the leading-order (uniform) term in the Taylor series is retained, a homogeneous "effective" Cosserat material can do so when two terms in the Taylor series are retained, when the material heterogeneities are less stiff than the matrix material. The result is a simple homogeneous material model that more accurately represents actual (compliant-inclusion-type) heterogeneous material response under slowly varying applied loading.

2 Review of Homogenization Results for Uniform Applied Loading

Here we briefly summarize well-known results for the effective moduli of a homogeneous, isotropic linear elastic matrix containing a dilute suspension of homogeneous, isotropic linear elastic inclusions having in general different moduli than the matrix; the inclusions are either cylinders (for plane strain deformations) or spheres (for three-dimensional deformations). As noted in Sec. 1, one approach for deriving such moduli is to require that they relate average (uniform) stress and strain in the same way that these quantities are related in the actual heterogeneous material. An alternative, equivalent approach for their derivation is to require that the total elastic energy in the uniform "effective" medium equals that in the actual heterogeneous medium under uniform applied loading. We will employ this energy approach in the present work.

When the composite is dilute, as considered here, we may employ the solution for an infinite body containing a single inclusion and subjected to uniform far-field loading. From this solution, we select a finite region containing the inclusion, and calculate the mean stresses acting on it. The effective moduli may then be calculated by equating, through first order in volume fraction, the elastic energy contained in the selected finite region calculated from the actual heterogeneous material solution with that calculated from a homogeneous effective body of the same size subjected to the mean stresses calculated from the infinite-body solution. We define the effective shear modulus as $\bar{\mu}$ and bulk modulus as $\bar{\kappa}$ (for 3D, whereas $\bar{\kappa}=3-4\bar{\nu}$, with $\bar{\nu}$ denoting in-plane Poisson's ratio for plane strain 2D). A sketch of this procedure is shown in Fig. 1, for plane strain deformation of an infinite plane with a circular hole.

Eshelby [8] and independently Hashin [9] have obtained the following effective elastic moduli for the three-dimensional problem of a matrix containing spherical inclusions (here retaining terms through first order in the volume fraction f of the inclusion phase)

$$\bar{\mu}=\mu_m+f\frac{5\mu_m(\mu_i-\mu_m)(3\kappa_m+4\mu_m)}{2(\mu_i+\mu_m)(3\kappa_m+4\mu_m)+\mu_m(3\kappa_m+4\mu_i)}$$

$$\bar{\kappa}=\kappa_m+f(\kappa_i-\kappa_m)\frac{3\kappa_m+4\mu_m}{3\kappa_i+4\mu_m} \tag{1}$$

where subscripts m and i denote matrix and inclusion, respectively.

In two-dimensional (plane strain) elasticity, the spheres are replaced by parallel infinite circular cylinders and the effective-modulus formulae through $O(f)$ are [10]

$$\bar{\mu}=\mu_m+f(1+\kappa_m)\mu_m\frac{\mu_i-\mu_m}{\kappa_m\mu_i+\mu_m}$$

$$\bar{\kappa}=\kappa_m+f(1+\kappa_m)\left[(\kappa_m-1)\frac{\mu_i-\mu_m}{\kappa_m\mu_i+\mu_m}-\frac{(\kappa_m-1)\mu_i-(\kappa_i-1)\mu_m}{2\mu_i+(\kappa_i-1)\mu_m}\right] \tag{2}$$

where now $\kappa=3-4\nu$, with ν denoting (in-plane) Poisson's ratio.

3 Homogenization Under Nonuniform Applied Loading

3.1 Taylor Series Representation of Slowly Varying Applied Loading. Let us consider an infinite body of composite material with a *dilute* distribution of inclusions, subjected to arbitrary but slowly varying far-field ("boundary") conditions. The far-field displacement field $\mathbf{u}(\mathbf{x})$ can then be expanded in a Taylor series about the location of the center of an inclusion (chosen as the origin of coordinates). Through second order, the most general representation for this is

$$u_i = \alpha_{ij} x_j + \beta_{ijk} x_j x_k \tag{3}$$

where α_{ij} and β_{ijk} are constant coefficients, the latter having the obvious symmetry $\beta_{ijk}=\beta_{ikj}$ (since x_j and x_k play the same role), indices range between 1 and 3 (1 and 2 for plane strain), and the usual summation convention for repeated indices is employed here and throughout the paper except where noted. Although coefficients α_{ij} are unrestricted, the quadratic part of the displacement field must satisfy the Navier equations of equilibrium without body forces, resulting in the following three (two for plane strain) restrictions

$$\beta_{kki} = -(1-2\nu_m)\beta_{ikk} \tag{4}$$

As is well known, the homogeneous effective Cauchy-elastic material, Eqs. (1) and (2), accurately mimics the response of a heterogeneous Cauchy material when this is subjected to a linearly varying displacement (uniform applied loading). However, in most practical situations, a composite material is subjected to a spatially varying applied loading. How well does the homogeneous effective Cauchy material mimic the actual heterogeneous one in this case, and can a homogeneous Cosserat material do better? Let us consider plane strain and three-dimensional deformations separately.

3.2 Plane Strain. Employing the constraint Eq. (4) and explicitly exhibiting the plane-strain bending contributions, the quadratic terms in the remote displacement field Eq. (3) become

$$u_1 = \left[\tilde{\beta}_{13} - \frac{\nu_m}{2(1-\nu_m)R_{23}}\right]x_1^2 + \frac{x_1 x_2}{R_{13}} - \left(2\frac{1-\nu_m}{1-2\nu_m}\tilde{\beta}_{13} + \frac{1}{2R_{23}}\right)x_2^2$$

$$u_2 = \left[\tilde{\beta}_{23} - \frac{\nu_m}{2(1-\nu_m)R_{13}}\right]x_2^2 + \frac{x_1 x_2}{R_{23}} - \left(2\frac{1-\nu_m}{1-2\nu_m}\tilde{\beta}_{23} + \frac{1}{2R_{13}}\right)x_1^2,$$

$$u_3 = 0 \tag{5}$$

where coefficients $\tilde{\beta}_{13}$, $\tilde{\beta}_{23}$ (index 3 denotes the out-of-plane direction and the others the nonnull displacement component directions) and bending curvatures R_{13} and R_{23} (index 3 again denotes the out-of-plane direction, while the other indices denote the directions of the normal components of bending stress) are arbitrary. Displacements Eqs. (5) a priori satisfy the Navier equations and thus represent the most general equilibrium plane-strain quadratic displacement field.

The problem of an infinite sheet containing a circular hole and subjected to far-field bending was solved by Muskhelishvili [11], and by Sendeckyj [12] in the general case of a circular elastic inclusion. The elastic fields produced by the far-field loading modes associated with $\tilde{\beta}_{13}$ and $\tilde{\beta}_{23}$ in an infinite sheet containing a circular elastic inclusion are determined in Appendix B (where the bending solution is also included for completeness). The important point with respect to our upcoming accurate modeling of effective material response is that *these solutions show* that the displacement field Eq. (5), valid exactly for a homogeneous material, is perturbed by the inclusion, in the material outside the inclusion, only by terms of $O(f^2)$.

3.3 Three-Dimensional Deformations. The most general quadratic equilibrium remote displacement field can be written as, using Eq. (3) with Eq. (4) (summation *not* implied for repeated indices)

$$u_i = \frac{x_i x_j}{R_{ik}} + \frac{x_i x_k}{R_{ij}} - \frac{1}{2R_{jk}}\left(x_j^2 + \frac{\nu_m}{1-\nu_m}x_i^2\right) - \frac{1}{2R_{kj}}\left(x_k^2 + \frac{\nu_m}{1-\nu_m}x_i^2\right)$$
$$+ (\Theta_j - \Theta_k)x_j x_k + (\tilde{\beta}_{ik} + \tilde{\beta}_{ij})x_i^2 - 2\frac{1-\nu_m}{1-2\nu_m}(\tilde{\beta}_{ik}x_j^2 + \tilde{\beta}_{ij}x_k^2) \tag{6}$$

where indices i, j, k are cyclic permutations of 1, 2, 3 (i.e., 1,2,3; 2,3,1; 3,1,2), illustrating the fact that the kinematics are the sum of six plane strain modes (defined by bending curvatures R_{ij} and additional free coefficients $\tilde{\beta}_{ij}$ (where i denotes the direction of the bending stress or non-null displacement component and j the out-of-plane direction)) and three torsional angles of twist/length Θ_i $(i=1,2,3)$. Therefore, the plane-strain displacement field Eq. (5) can be obtained from Eq. (6) by taking $1/R_{12}=1/R_{21}=1/R_{32}=1/R_{31}=\tilde{\beta}_{12}=\tilde{\beta}_{21}=\tilde{\beta}_{32}=\tilde{\beta}_{31}=\Theta_1=\Theta_2=\Theta_3=0$.

The problem of an infinite elastic matrix containing a spherical void and subjected to remote bending loading (a particular case of Eq. (6) in which all $\tilde{\beta}_{ij}$ and Θ_i are zero) has been solved by Sen [13], and by Das [14] for the general case of a spherical elastic inclusion. These solutions show that the bending displacement field, valid exactly for a homogeneous material, is perturbed by the inclusion in the region outside the inclusion by terms of $O(f^{5/3})$. The fact that the perturbation remains at $O(f^{5/3})$ for the general quadratic displacement field Eq. (6) is shown in Appendix C, where the solution for a spherical elastic inclusion in an infinite elastic matrix, subject to the remote displacement field Eq. (6) is obtained. Appendix C also shows that the Das [14] solution is incomplete, and that it can be expressed purely in terms of simple functions.

3.4 Conclusion. The *quadratic* part of the displacement field Eq. (3), together with equilibrium requirements Eq. (4), which is valid exactly for a homogeneous material, is perturbed by a cylindrical or spherical inclusion in the region outside the inclusion by terms of $O(f^2)$ for two-dimensional elasticity and $O(f^{5/3})$ for three-dimensional elasticity.

In other words, in an asymptotic expansion in inclusion volume fraction f of the displacement field solution outside the inclusion, through order f the inclusion is neutral under remote quadratic displacement conditions. Therefore, the effective moduli determined under the remote quadratic displacement conditions are identical (to first order in f) with the moduli of the matrix material.

4 Standard Homogenized Material is in Error for Quadratic Applied Displacements

Now we are in a position to face the main problem, namely: under an applied *linear* remote displacement field (*uniform* applied remote stress) the perturbation induced by the inclusion in the displacement field solution in the surrounding matrix material is $O(f)$, while under an applied *quadratic* remote displacement field (applied *linear* remote stress field) the perturbation in the displacement field solution in the matrix becomes $O(f^{5/3})$ for 3D and $O(f^2)$ for 2D elasticity.

Therefore, *the effective material defined by Eqs. (1) and (2) is stiffer (more compliant) for linearly varying applied loading than the actual heterogeneous material for inclusions stiffer (more compliant) than the matrix.* That is, if the heterogeneous material (matrix with inclusion) is represented in the usual way in composite materials theory—by a homogeneous material with effective moduli given by Eqs. (1) or (2)—this representation works well for uniform applied loading, but for linearly varying applied stress, it is in error by terms of $O(f)$.

To better elucidate this point, let us consider a cube of edge h, composed of a homogeneous effective material having properties Eqs. (1) or (2) and subject to the quadratic displacement field Eqs. (5) or (6). The total elastic energy in such a cube is obtained by calculating the strain energy density from Eqs. (5) or (6) and then integrating this over the cube.

The total elastic energy in the cube, $\mathcal{E}$, is, for plane strain

$$\mathcal{E}_{\text{Cauchy}} = \frac{h^5\bar{\mu}}{12(1-\bar{\nu})}\left(\frac{1}{R_{13}^2}+\frac{1}{R_{23}^2}\right)+\frac{h^5\bar{\mu}(1-\bar{\nu})(3-4\bar{\nu})}{3(1-2\bar{\nu})^2}(\tilde{\beta}_{13}^2+\tilde{\beta}_{23}^2)$$
$$= h^5\mu_m\left(\frac{1}{R_{13}^2}+\frac{1}{R_{23}^2}\right)\left(\frac{1}{12(1-\nu_m)}-\Xi_R f\right)+h^5\mu_m(\tilde{\beta}_{13}^2+\tilde{\beta}_{23}^2)\left[\frac{(1-\nu_m)(3-4\nu_m)}{3(1-2\nu_m)^2}-\Xi_\beta f\right]+O(f^2) \tag{7}$$

where

$$\Xi_R = \frac{1}{12(1-\nu_m)}\left[\frac{3\mu_m+\mu_i(1-4\nu_m)}{\mu_m+\mu_i(3-4\nu_m)}-\frac{2\mu_i(1-\nu_m)}{\mu_i+\mu_m(1-2\nu_i)}\right]$$

$$\Xi_\beta = -\frac{(1-\nu_m)(3-4\nu_m)}{3(1-2\nu_m)^2}\left(\frac{2\mu_i(1-\nu_m)(5-6\nu_m)}{(1-2\nu_m)(3-4\nu_m)[\mu_i+\mu_m(1-2\nu_i)]}\right.$$
$$\left.+\frac{\mu_i\{-13+2\nu_m[9+4(3-4\nu_m)\nu_m]\}+\mu_m\{-7+2\nu_m[13-8\nu_m(3-2\nu_m)]\}}{(1-2\nu_m)(3-4\nu_m)[\mu_m+\mu_i(3-4\nu_m)]}\right) \tag{8}$$

while for three-dimensional deformation it is

$$\mathcal{E}_{\text{Cauchy}} = \frac{h^5\bar{\mu}}{12(1-\bar{\nu})}\sum_{\substack{i,j=1\\ i\neq j}}^{3}\left(\frac{1}{R_{ij}^2}+\frac{\bar{\nu}}{R_{ij}R_{ji}}\right)+\frac{h^5\bar{\mu}}{12}\left(\sum_{i=1}^{3}\Theta_i^2-\frac{1}{2}\sum_{\substack{i,j=1\\ i\neq j}}^{3}\Theta_i\Theta_j\right)+\frac{2h^5\bar{\mu}(1-\bar{\nu})}{3(1-2\bar{\nu})}\left[\tilde{\beta}_{12}\tilde{\beta}_{13}+\tilde{\beta}_{21}\tilde{\beta}_{23}+\tilde{\beta}_{31}\tilde{\beta}_{32}+\frac{3-4\bar{\nu}}{2(1-2\bar{\nu})}\sum_{\substack{i,j=1\\ i\neq j}}^{3}\tilde{\beta}_{ij}^2\right]$$
$$= h^5\mu_m\sum_{\substack{i,j=1\\ i\neq j}}^{3}\frac{1}{R_{ij}^2}\left[\frac{1}{12(1-\nu_m)}-\Xi_R f\right]+h^5\mu_m\sum_{\substack{i,j=1\\ i\neq j}}^{3}\frac{1}{R_{ij}R_{ji}}\left[\frac{\nu_m}{12(1-\nu_m)}-\Xi_{RR} f\right]+h^5\mu_m\left(\sum_{i=1}^{3}\Theta_i^2-\frac{1}{2}\sum_{\substack{i,j=1\\ i\neq j}}^{3}\Theta_i\Theta_j\right)\left(\frac{1}{12}-\Xi_\Theta f\right)$$
$$+h^5\mu_m\sum_{\substack{i,j=1\\ i\neq j}}^{3}\tilde{\beta}_{ij}^2\left[\frac{(1-\nu_m)(3-4\nu_m)}{3(1-2\nu_m)^2}-\Xi_\beta f\right]+h^5\mu_m(\tilde{\beta}_{12}\tilde{\beta}_{13}+\tilde{\beta}_{21}\tilde{\beta}_{23}+\tilde{\beta}_{31}\tilde{\beta}_{32})\left[\frac{2(1-\nu_m)}{3(1-2\nu_m)}-\Xi_{\beta\beta} f\right]+O(f^{5/3}) \tag{9}$$

where

$$\Xi_R = \frac{1}{2(1-\nu_m)}-\frac{28\mu_i^2+34\mu_i\mu_m+13\mu_m^2}{4(2\mu_i+\mu_m)[\mu_m(7-5\nu_m)+2\mu_i(4-5\nu_m)]}-\frac{\mu_m(2\mu_i-\mu_m)(1-2\nu_i)+2\mu_i^2(1+\nu_i)}{4(2\mu_i+\mu_m)[\mu_i(1+\nu_i)+2\mu_m(1-2\nu_i)]}$$

$$\Xi_{RR} = \frac{1}{2(1-\nu_m)}-\frac{26\mu_i^2+38\mu_i\mu_m+11\mu_m^2}{4(2\mu_i+\mu_m)[\mu_m(7-5\nu_m)+2\mu_i(4-5\nu_m)]}-\frac{(\mu_i+\mu_m)\mu_i(1+\nu_i)+\mu_m^2(1-2\nu_i)}{4(2\mu_i+\mu_m)[\mu_i(1+\nu_i)+2\mu_m(1-2\nu_i)]}$$

$$\Xi_\Theta = \frac{5(\mu_m-\mu_i)(1-\nu_m)}{4\mu_m(7-5\nu_m)+8\mu_i(4-5\nu_m)}$$

$$\Xi_{\beta\beta} = -\frac{2(1-\nu_m)}{[2\mu_m(1-2\nu_i)+\mu_i(1+\nu_i)](1-2\nu_m)^2[\mu_m(7-5\nu_m)+\mu_i(8-10\nu_m)]}\{2\mu_i^2(1+\nu_i)(1-2\nu_m)(3-5\nu_m)+\mu_i\mu_m(1-5\nu_m)[3-4\nu_m$$
$$-\nu_i(9-14\nu_m)]-\mu_m^2(1-2\nu_i)[9-\nu_m(26-25\nu_m)]\}$$

$$\Xi_\beta = \frac{(1-\nu_m)}{[\mu_m(7-5\nu_m)+2\mu_i(4-5\nu_m)](1-2\nu_m)^3[2\mu_m(1-2\nu_i)+\mu_i(1+\nu_i)]}\{2\mu_i^2(1+\nu_i)(-10+53\nu_m-91\nu_m^2+50\nu_m^3)+\mu_m^2(1-2\nu_i)(25$$
$$-104\nu_m+181\nu_m^2-110\nu_m^3)-\mu_i\mu_m[5-73\nu_m+164\nu_m^2-100\nu_m^3+\nu_i(5+149\nu_m-454\nu_m^2+320\nu_m^3)]\} \tag{10}$$

For two-dimensional deformations the terms Ξ_R and Ξ_β, while for three-dimensional deformations the terms $(\Xi_R-|\Xi_{RR}|)$, $(2\Xi_\beta-|\Xi_{\beta\beta}|)$, and Ξ_Θ, are *all negative* for inclusions stiffer than the matrix (i.e., when the energy of a composite specimen is higher than that of the same specimen comprised of purely matrix material), all zero when they have the same stiffness, and *all positive* for inclusions less stiff than the matrix. This will be in a sense used as our definition of "inclusion stiffer than the matrix."

If the elastic energy Eq. (9) (or Eq. (7)) is compared to that evaluated for an identical prism now comprised of matrix material and containing a spherical (cylindrical in 2D) inclusion, ideally removed from an infinite body that is subjected to the far-field quadratic displacements Eq. (6) (or Eq. (5)), there is a mismatch of the linear terms in f, so that homogenization yields a material stiffer (more compliant) than the heterogeneous solution, for an inclusion stiffer (more compliant) than the matrix.

5 Comparison With Cosserat Material

The key point in the above discussion is that the results for the heterogeneous material are compared to a homogeneous linear elastic material, providing the effective properties. While a homogeneous material with appropriately chosen effective moduli can successfully mimic the composite material when uniform stress fields are applied, we showed that it cannot do so when the simplest nonuniform (i.e., uniform plus linearly varying) stress field is applied. What happens now if this comparison is made between a

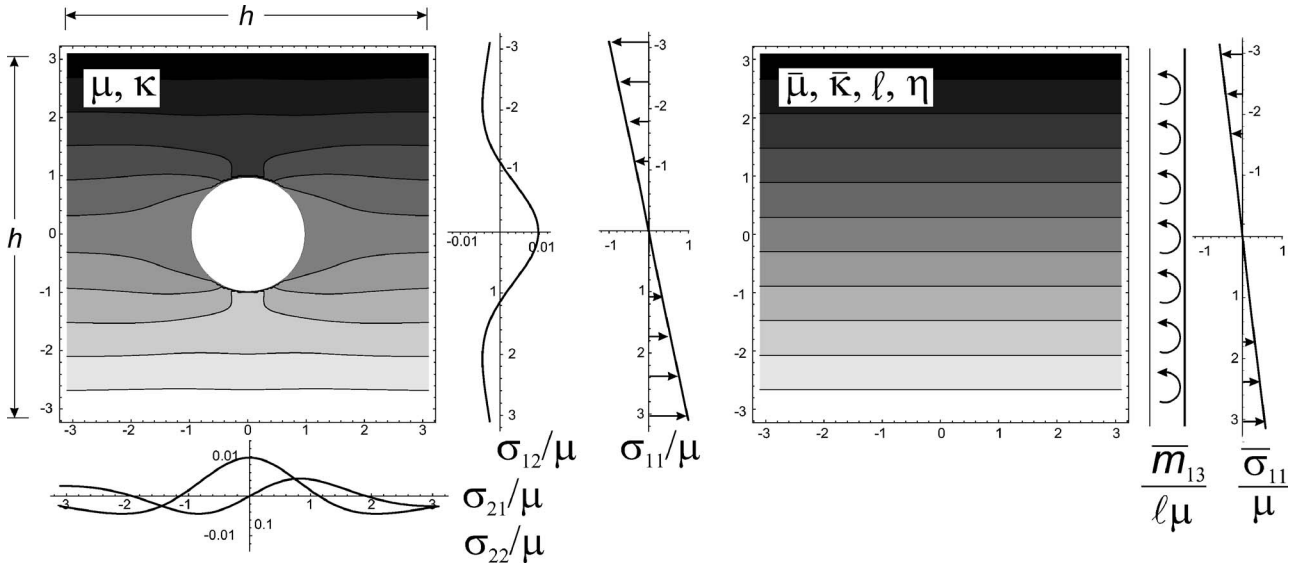

Fig. 2 Procedure of homogenization of a material containing a dilute distribution of circular voids and subject to a far-field bending stress distribution. Heterogeneous material (left) is an $h\times h$ prism removed from an infinite sheet that is subjected to uniaxial, linearly varying far-field stress; homogeneous Cosserat-elastic material (right) subject to the same mean moment (produced by $\bar{m}_{13}$ and $\bar{\sigma}_{11}$) calculated from the heterogeneous prism. For the plane strain problem (where η does not appear), level sets of σ_{11} are shown; note that the values of σ_{12}, σ_{21}, and σ_{22}, shown parallel to the edges, are less than 1/100 of the maximum value of σ_{11} at a distance from inclusion center equal to three times the radius of the inclusion (contrast this with the order of the effect in Fig. 1).

composite material and a homogeneous Cosserat or micropolar material? Note that this question has fundamental—as opposed to empirical—motivation: the assumption leading to standard Cauchy elasticity—that surface resultant moments/area vanish as the Cauchy tetrahedron becomes vanishing small—is a sensible approximation for materials with extremely small-scale microstructure, but is not in general otherwise justifiable. Absent this assumption, a Cosserat-type constitutive framework arises.

5.1 Simplest Cosserat Constitutive Model. We begin for simplicity with constrained-rotation micropolar materials (the simplest Cosserat constitutive model), for which the constitutive equations are [15]

$$\sigma_{ij}=2\mu\left(\varepsilon_{ij}+\frac{\nu}{1-2\nu}\varepsilon_{kk}\delta_{ij}\right),\quad m_{ij}=4\mu\ell^2(\chi_{ji}+\eta\chi_{ij}) \tag{11}$$

where σ_{ij} is the symmetric part of the force-stress tensor; ε_{ij} is the infinitesimal strain tensor; m_{ij} is the deviator of the couple-stress tensor; and χ_{ij} is the torsion-flexure tensor. The kinematical quantities are defined in terms of the displacement field u_i as

$$\varepsilon_{ij}=\tfrac{1}{2}(u_{i,j}+u_{j,i}),\quad \chi_{ij}=\omega_{i,j}=\tfrac{1}{2}e_{ihk}u_{k,hj} \tag{12}$$

where e_{ihk} is the Ricci (permutation) tensor; ω_i is the macrorotation axial vector; and a subscript comma denotes partial differentiation with respect to subsequent indices. The material parameters ν and μ appearing in Eq. (11) are the usual (Poisson and shear) elastic moduli (subject to the usual restrictions), whereas material parameters ℓ and η define the Cosserat behavior; in particular, the former is a characteristic length of the material and the latter is dimensionless and subject to the restriction $-1<\eta<1$ for positive definiteness of the strain energy.

Let us consider now two ideal material elements: a cube of edges h of Cauchy-elastic material containing an inclusion, ideally removed from an infinite body that is subjected to far-field loading, and the same cube instead composed of a homogeneous, constrained-rotation Cosserat material, Eqs. (11). We wish to determine the values of the effective Cosserat moduli $\bar{\mu}$, $\bar{\nu}$, ℓ, and η so that the homogeneous Cosserat material best mimics the heterogeneous Cauchy material under general slowly varying applied loading (Fig. 2, illustrating for simplicity a bending stress distribution).

5.2 Matching With the Uniform Stress Field. For *uniform* applied stress (and zero applied couple stress) the effective modulus values Eqs. (1) and (2), identical to those obtained for Cauchy-elastic material, are found for the Cosserat material. The reason for this is simply that for a uniform applied stress on the Cosserat material, a homogeneous deformation with null deformation-curvature tensor is produced, so that the Cosserat effects disappear (i.e., the moduli ℓ and η do not enter the solution).

5.3 Matching With Linearly Varying Remote Stress Field. For a linearly varying remote applied stress on the Cosserat material, Cosserat effects are present and, as will be shown, for inclusions less stiff than the matrix, they permit minimization, and for certain deformations elimination, of the mismatch in the strain energy between the actual composite material and the homogeneous effective Cosserat material.

Boundary conditions for a Cosserat solid and a Cauchy-elastic solid are not equivalent. For instance, in a purely kinematic approach, for a Cosserat material we can prescribe displacements Eqs. (6) (or Eqs. (5)) along a side of the prism, but the two tangential components of the rotation must also be specified, the latter not being necessary in a Cauchy solid. Following the kinematic approach, we assume displacements Eqs. (6) (or Eqs. (5)), and *the rotations deduced from these displacements*, to be prescribed along all sides of the prism for the Cosserat material. (For the Cauchy material, only the displacements Eqs. (6) (or Eqs. (5)) are prescribed on the boundary, but the resulting solution has rotations there identical to those prescribed for the Cosserat material, so the Cosserat and Cauchy material solutions correspond to exactly the same problem.) The solution to this boundary value problem for pure bending of the Cosserat material was given by Koiter ([15], his Secs. 6.2 and 6.3).

Generalizing the Koiter solution, for the displacement field Eq. (6) (or Eq. (5)), with ν_m replaced by $\bar{\nu}$, the non-null kinematical quantities become

$$\varepsilon_{ii} = \frac{x_j}{R_{ik}} + \frac{x_k}{R_{ij}} - x_i \frac{\bar{\nu}}{1-\bar{\nu}}\left(\frac{1}{R_{jk}} + \frac{1}{R_{kj}}\right) + 2x_i(\tilde{\beta}_{ij} + \tilde{\beta}_{ik})$$

(indices not summed; i,j,k cyclic),

$$\varepsilon_{ij} = -2\frac{1-\bar{\nu}}{1-2\bar{\nu}}(x_j\tilde{\beta}_{ik} + x_i\tilde{\beta}_{jk}) - e_{ijk}x_k\frac{\Theta_i - \Theta_j}{2}$$

(indices not summed and all different),

$$\chi_{ij} = \frac{1}{2}\delta_{ij}\left(3\Theta_i - \sum_{k=1}^{3}\Theta_k\right) + e_{jik}\left(\frac{1}{R_{ji}} + 2\tilde{\beta}_{ki}\frac{1-\bar{\nu}}{1-2\bar{\nu}}\right) \tag{13}$$

(indices not summed).

The total strain energy in the cube is thus

$$\mathcal{E} = \mathcal{E}_{\text{Cauchy}} + 2h^3\bar{\mu}\ell^2(\chi_{ij}\chi_{ij} + \eta\chi_{ji}\chi_{ij}) \tag{14}$$

where

$$\chi_{ij}\chi_{ij} = \frac{3}{2}\left(\sum_{i=1}^{3}\Theta_i^2 - \frac{1}{2}\sum_{\substack{i,j=1\\ i\neq j}}^{3}\Theta_i\Theta_j\right) + \sum_{\substack{i,j,k=1\\ i\neq j\neq k}}^{3}\left(\frac{1}{R_{ij}} + 2\tilde{\beta}_{kj}\frac{1-\bar{\nu}}{1-2\bar{\nu}}\right)^2 \tag{15}$$

and

$$\chi_{ji}\chi_{ij} = \frac{3}{2}\left(\sum_{i=1}^{3}\Theta_i^2 - \frac{1}{2}\sum_{\substack{i,j=1\\ i\neq j}}^{3}\Theta_i\Theta_j\right) - \sum_{\substack{i,j,k=1\\ i\neq j\neq k}}^{3}\left(\frac{1}{R_{ij}} + 2\tilde{\beta}_{kj}\frac{1-\bar{\nu}}{1-2\bar{\nu}}\right)\left(\frac{1}{R_{ji}} + 2\tilde{\beta}_{ki}\frac{1-\bar{\nu}}{1-2\bar{\nu}}\right) \tag{16}$$

which, for plane-strain deformations in the x_1, x_2 plane become

$$\chi_{ij}\chi_{ij} = \left(\frac{1}{R_{23}} + 2\tilde{\beta}_{13}\frac{1-\bar{\nu}}{1-2\bar{\nu}}\right)^2 + \left(\frac{1}{R_{13}} + 2\tilde{\beta}_{23}\frac{1-\bar{\nu}}{1-2\bar{\nu}}\right)^2, \quad \chi_{ji}\chi_{ij} = 0 \tag{17}$$

5.4 Result 1. The nonpolar (i.e., standard effective Cauchy) case is obtained from the strain energy Eq. (14) by setting the internal length equal to zero, $\ell = 0$; therefore, since ℓ enters Eq. (14) only as ℓ^2, and since its coefficient cannot be negative for allowable modulus values, *the strain energy for the effective Cosserat material is never less than the strain energy for the effective Cauchy material.* This means that the introduction of Cosserat effects can only *increase* the strain energy of the effective material and therefore can only be useful when coefficients Ξ_R and Ξ_β are positive in plane strain (in Eqs. (7)) or when $\Xi_R - |\Xi_{RR}| > 0$, $2\Xi_\beta - |\Xi_{\beta\beta}| > 0$, and $\Xi_\Theta > 0$, in 3D (in Eqs. (9)), i.e., *for inclusions less stiff than the matrix*. In the case of an inclusion stiffer than the matrix, Cosserat effects make the homogenized material even stiffer than the already overly stiff effective Cauchy material resulting from homogenization for uniform stress. For these situations the simple Cosserat effective material cannot provide an improvement to the standard Cauchy effective material.

5.5 Result 2 for 2D Deformations. Let us begin with the two-dimensional (plane strain) formulation, where there is only one remaining undetermined parameter, the internal characteristic length ℓ, in the elastic energy, Eq. (14) (parameter η only enters the elastic energy in the three-dimensional case). We seek the ℓ value that permits minimization of the elastic energy difference through $O(f)$, for arbitrary equilibrium quadratic displacement remote boundary conditions, between the heterogeneous Cauchy material (whose energy has no $O(f)$ term) and the homogeneous effective Cosserat material:

$$\mathcal{E}_{\text{Cauchy}}(\mu_m, \nu_m) - [\mathcal{E}_{\text{Cauchy}}(\bar{\mu}, \bar{\nu}) + 2h^3\bar{\mu}\ell^2\chi_{ij}\chi_{ij}] \tag{18}$$

which is (having divided by h^5)

$$\frac{\mu_m}{12(1-\nu_m)}\left(\frac{1}{R_{13}^2} + \frac{1}{R_{23}^2}\right) + \frac{\mu_m(1-\nu_m)(3-4\nu_m)}{3(1-2\nu_m)^2}(\tilde{\beta}_{13}^2 + \tilde{\beta}_{23}^2) - \left\{\frac{\bar{\mu}}{12(1-\bar{\nu})}\left(\frac{1}{R_{13}^2} + \frac{1}{R_{23}^2}\right) + \frac{\bar{\mu}(1-\bar{\nu})(3-4\bar{\nu})}{3(1-2\bar{\nu})^2}(\tilde{\beta}_{13}^2 + \tilde{\beta}_{23}^2) + 2\bar{\mu}\frac{\ell^2}{h^2}\left[\left(\frac{1}{R_{23}} + 2\tilde{\beta}_{13}\frac{1-\bar{\nu}}{1-2\bar{\nu}}\right)^2 + \left(\frac{1}{R_{13}} + 2\tilde{\beta}_{23}\frac{1-\bar{\nu}}{1-2\bar{\nu}}\right)^2\right]\right\} \tag{19}$$

We wish to use ℓ to increase the elastic energy of the effective Cosserat material in such a way that this becomes closer to the correct value $\mathcal{E}_{\text{Cauchy}}(\mu, \nu)$, but without exceeding this value for any value of the *free parameters* defining the deformation modes: $1/R_{13}$, $1/R_{23}$, $\tilde{\beta}_{13}$, and $\tilde{\beta}_{23}$. Therefore, employing Eq. (7), Eq. (19) can be written as, retaining only terms through $O(f)$

$$\left(\frac{1}{R_{13}^2} + \frac{1}{R_{23}^2}\right)\Xi_R f + (\tilde{\beta}_{13}^2 + \tilde{\beta}_{23}^2)\Xi_\beta f - 2\frac{\ell^2}{h^2}\left[\left(\frac{1}{R_{23}} + 2\tilde{\beta}_{13}\frac{1-\nu_m}{1-2\nu_m}\right)^2 + \left(\frac{1}{R_{13}} + 2\tilde{\beta}_{23}\frac{1-\nu_m}{1-2\nu_m}\right)^2\right] \geq 0 \tag{20}$$

and the problem is to find an ℓ^2/h^2 such that Eq. (20) is satisfied for all $1/R_{13}$, $1/R_{23}$, $\tilde{\beta}_{13}$, and $\tilde{\beta}_{23}$, coming as close to equality as possible. Note that, since the term multiplying ℓ^2 is always negative, inequality (20) can be satisfied only for inclusions less stiff than the matrix, i.e., when Ξ_R and Ξ_β are both positive.

Now, problem (20) can be transformed into the form $\mathbf{xAx} \geq 0$, with vector $\{\mathbf{x}\} = \{1/R_{13}, \tilde{\beta}_{23}, 1/R_{23}, \tilde{\beta}_{13}\}$, so that it becomes equivalent to the requirement of positive semi-definiteness of the 4×4 matrix $\mathbf{A}$ (which is composed of two identical 2×2 blocks, while all other entries are null). This matrix has two distinct eigenvalues with double multiplicity; requiring that the smaller eigenvalue be zero yields

$$\frac{\ell^2}{h^2} = \frac{f}{\left(\frac{1-\nu_m}{1-2\nu_m}\right)^2\frac{8}{\Xi_\beta} + \frac{2}{\Xi_R}} \tag{21}$$

valid only for both Ξ_R and Ξ_β positive.

Obviously, the meaning of negative values of ℓ^2 is merely that the inclusion is stiffer than the matrix and no (real) value exists for the characteristic length that will permit the elastic energies to match. In such cases, $\ell = 0$ gives the smallest difference between the energies. Using $f = \pi a^2/h^2$, Eq. (21) becomes

$$\ell = a\sqrt{\frac{\pi}{\frac{8(1-\nu_m)^2}{(1-2\nu_m)^2\Xi_\beta} + \frac{2}{\Xi_R}}} \tag{22}$$

valid only for both Ξ_R and Ξ_β positive. Note from Eq. (22) that $\ell = 0$ when $a = 0$, but that ℓ/a is independent of f (under our assumption of small f). Note that in the limit of an incompressible matrix, $\nu_m = 1/2$, Eq. (22) reduces to

$$\ell = a\sqrt{\frac{\pi\Xi_R}{2}} \tag{23}$$

showing that the corresponding applied deformation mode is a pure bending. In this case, in other words, the characteristic length Eq. (23) provides an exact match between the energies of the actual heterogeneous solid and the homogenized one under arbitrary uniform plus pure bending applied loading.

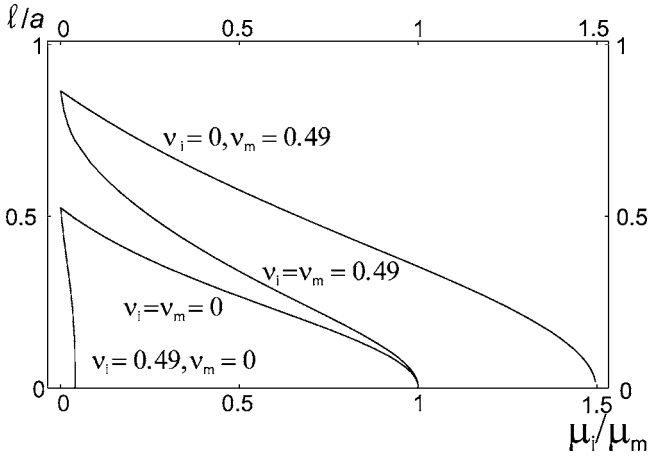

Fig. 3 Characteristic length divided by circular cylindrical inclusion radius for a homogeneous Cosserat material deduced from homogenization of a matrix containing a dilute distribution of parallel, infinite circular cylindrical inclusions (plane strain, Eq. (22))

In the extreme case when the inclusion is a void, Eq. (22) becomes

$$\ell = a\sqrt{\frac{\pi}{24(1-\nu_m)\left\{\frac{1}{3}+\frac{1-2\nu_m}{7-2\nu_m[13-8\nu_m(3-2\nu_m)]}\right\}}} \tag{24}$$

where the radical in Eq. (24) is always positive.

The characteristic length divided by the radius of the inclusion, ℓ/a, is plotted in Fig. 3 versus the contrast in the inclusion/matrix shear moduli, μ_i/μ_m. A null contrast corresponds to a void, Eq. (24). The different curves in the figure refer to different values of Poisson's ratios. The values of the curves at $\mu_i/\mu_m=0$ depend only on ν_m; curves are plotted for ν_m and ν_i each having values 0.49 and 0. Note also that for $\nu_m=\nu_i$, $\ell=0$ results for $\mu_i=\mu_m$, as it should.

For a sufficiently compliant inclusion, a positive characteristic length for an effective Cosserat material is always found, which decreases to zero at sufficiently high inclusion stiffness.

5.6 Result 2 for 3D Deformations. Let us now consider three-dimensional deformations. By introducing the symbol

$$T^2 = \sum_{i=1}^{3}\Theta_i^2 - \frac{1}{2}\sum_{\substack{i,j=1\\ i\neq j}}^{3}\Theta_i\Theta_j \tag{25}$$

the three-dimensional version of non-negativity of the energy difference Eq. (18) becomes

$$\sum_{\substack{i,j=1\\ i\neq j}}^{3}\frac{1}{R_{ij}^2}\Xi_R + \sum_{\substack{i,j=1\\ i\neq j}}^{3}\frac{1}{R_{ij}R_{ji}}\Xi_{RR} + T^2\Xi_\Theta + \sum_{\substack{i,j=1\\ i\neq j}}^{3}\tilde{\beta}_{ij}^2\Xi_\beta + (\tilde{\beta}_{12}\tilde{\beta}_{13} + \tilde{\beta}_{21}\tilde{\beta}_{23} + \tilde{\beta}_{31}\tilde{\beta}_{32})\Xi_{\beta\beta} - 2\frac{\bar{\mu}\ell^2}{\mu_m f h^2}\left[(1+\eta)\frac{3}{2}T^2 + \sum_{\substack{i,j,k=1\\ i\neq j\neq k}}^{3}\left(\frac{1}{R_{ij}} + 2\tilde{\beta}_{kj}\frac{1-\bar{\nu}}{1-2\bar{\nu}}\right)^2 - \eta\sum_{\substack{i,j,k=1\\ i\neq j\neq k}}^{3}\left(\frac{1}{R_{ij}} + 2\tilde{\beta}_{kj}\frac{1-\bar{\nu}}{1-2\bar{\nu}}\right)\left(\frac{1}{R_{ji}} + 2\tilde{\beta}_{ki}\frac{1-\bar{\nu}}{1-2\bar{\nu}}\right)\right] \geqslant 0 \tag{26}$$

Equation (26) depends on the arbitrary deformation modes. These are coupled in groups of four (each group entering in exactly the same way), plus T; for example, $1/R_{13}$, $1/R_{31}$, $\tilde{\beta}_{21}$, $\tilde{\beta}_{23}$ are coupled. Thus it is sufficient to consider these four parameters together with T, and take all others equal to zero. Doing this, Eq. (26) becomes, retaining only leading-order terms in f

$$\left(\frac{1}{R_{13}^2}+\frac{1}{R_{31}^2}\right)\Xi_R + \frac{2}{R_{13}R_{31}}\Xi_{RR} + T^2\Xi_\Theta + (\tilde{\beta}_{21}^2+\tilde{\beta}_{23}^2)\Xi_\beta + \tilde{\beta}_{21}\tilde{\beta}_{23}\Xi_{\beta\beta} - 2\frac{\ell^2}{fh^2}\left[(1+\eta)\frac{3T^2}{2} + \left(\frac{1}{R_{13}} + 2\tilde{\beta}_{23}\frac{1-\nu_m}{1-2\nu_m}\right)^2 + \left(\frac{1}{R_{31}} + 2\tilde{\beta}_{21}\frac{1-\nu_m}{1-2\nu_m}\right)^2 - 2\eta\left(\frac{1}{R_{13}} + 2\tilde{\beta}_{23}\frac{1-\nu_m}{1-2\nu_m}\right)\left(\frac{1}{R_{31}} + 2\tilde{\beta}_{21}\frac{1-\nu_m}{1-2\nu_m}\right)\right] \geqslant 0 \tag{27}$$

Equation (27) involves a quadratic form, so that it can be represented in matrix form as

$$\left[\Xi_\Theta - 3\frac{\ell^2}{fh^2}(1+\eta)\right]T^2 + \mathbf{x}\mathbf{A}\mathbf{x} \geqslant 0 \tag{28}$$

where vector $\{\mathbf{x}\}=\{1/R_{13}, 1/R_{31}, \tilde{\beta}_{21}, \tilde{\beta}_{23}\}$. Matrix $\mathbf{A}$ is a 4×4 block and the Condition (26), viewed as the condition of positive semi-definiteness of $\mathbf{A}$ (since the coefficient of T^2 must be $\geqslant0$), yields non-negativeness of four eigenvalues, plus non-negativity of the coefficient of T^2. Two of these conditions can be shown to be contained within the other two, from which two values of Cosserat length ℓ can be obtained to ensure positive semi-definiteness of $\mathbf{A}$. The minimum among these two lengths, plus that obtained considering T, yields the Cosserat length for Condition (26) to be satisfied

$$\ell(\eta) = af^{1/6}\left(\frac{4\pi}{3}\right)^{1/3} g(\mu_i, \mu_m, \nu_i, \nu_m, \eta) \tag{29}$$

where

$$g(\mu_i, \mu_m, \nu_i, \nu_m, \eta) = \min\left[\frac{\Xi_\Theta}{3(1+\eta)}, \frac{(1-2\nu_m)^2}{2(1+\eta)\left(\frac{8(1-\nu_m)^2}{2\Xi_\beta - \Xi_{\beta\beta}} + \frac{(1-2\nu_m)^2}{\Xi_R - \Xi_{RR}}\right)}, \frac{(1-2\nu_m)^2}{2(1-\eta)\left(\frac{8(1-\nu_m)^2}{2\Xi_\beta + \Xi_{\beta\beta}} + \frac{(1-2\nu_m)^2}{\Xi_R + \Xi_{RR}}\right)}\right]^{1/2} \tag{30}$$

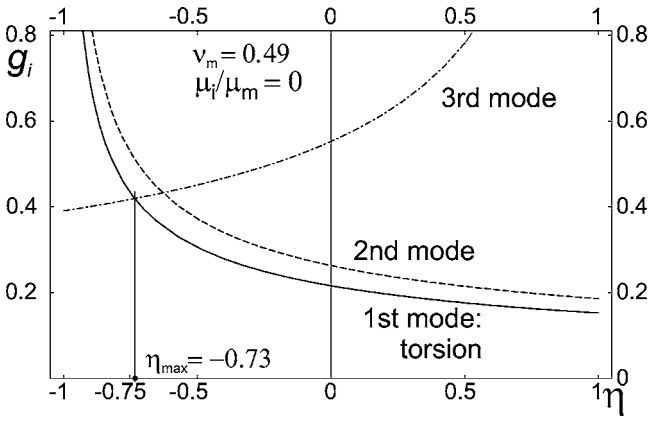

Fig. 4 The three functions g_i appearing in Eq. (30), among which the minimum is selected for given values of η

in which all terms are always non-negative for inclusions less stiff than the matrix. Equation (29) applies for given values of μ_i, μ_m, ν_i, ν_m, and η.

In Eq. (30), the minimum among the three functions (call them g_i) is taken. These functions have the typical dependence on η shown in Fig. 4, drawn for $\mu_i/\mu_m=0$ (so that the inclusion is a void) and $\nu_m=0.49$ (a case that will also be considered later). In this figure, one of the g_i's corresponds to the torsion mode, while the other two modes involve both bending and the modes described by the $\tilde{\beta}_{ij}$.

Since η is a constitutive parameter which can be chosen so that the effective Cosserat material best mimics the actual heterogeneous material's response, it is optimal to choose it so that the *Cosserat effective material matches the actual heterogeneous one for two modes of deformation*, which corresponds to the intersection of the two lower curves in Fig. 4, that is, to the largest of the minima (i.e., the supremum) of the three g_i's (corresponding to $\eta_{\max}$ in the figure). Therefore

$$\ell = af^{1/6}\left(\frac{4\pi}{3}\right)^{1/3} \sup_{\eta\in(-1,1)} g(\mu_i,\mu_m,\nu_i,\nu_m,\eta) \tag{31}$$

The case of an incompressible matrix ($\nu_m \to 1/2$) is worth noting. In this case, Eq. (30) becomes

$$g(\mu_i,\mu_m,\nu_i,\nu_m,\eta) = \min\left[\frac{\Xi_\Theta}{3(1+\eta)},\ \frac{\Xi_R-\Xi_{RR}}{2(1+\eta)},\ \frac{\Xi_R+\Xi_{RR}}{2(1-\eta)}\right]^{1/2} \tag{32}$$

showing that bending and torsion are the only modes entering the formula. In this case, in other words, the characteristic length ℓ and parameter η found from Eq. (31), in which Eq. (32) is used for function g, provide an exact match between the energies of the actual heterogeneous solid and the homogenized Cosserat one under arbitrary uniform plus bending and torsion applied loading.

The limit $\mu_i \to 0$ of Eq. (31) yields the case of a spherical void

$$\ell = af^{1/6}\frac{\sqrt[3]{4\pi/3}}{\sqrt{7-5\nu_m}} \max_{\eta\in(-1,1)} \min\left(\frac{5(1-\nu_m)}{12(1+\eta)},\ \frac{5(1-\nu_m)[4-\nu_m(11-15\nu_m)]}{4[13-\nu_m(37-40\nu_m)](1+\eta)},\ \frac{(1+\nu_m)\{17-\nu_m[74-\nu_m(129-80\nu_m)]\}}{2(1-\nu_m)\{21-\nu_m[78-\nu_m(121-80\nu_m)]\}(1-\eta)}\right)^{1/2} \tag{33}$$

In the case of matrix incompressibility, $\nu_m \to 1/2$, Eq. (33) becomes

$$\ell = af^{1/6}\frac{\sqrt[3]{4\pi/3}}{6}\sqrt{\frac{41}{6}}, \quad \eta = -\frac{31}{41} \tag{34}$$

in which case both the bending and the torsion modes are simultaneously matched.

We emphasize with respect to all the above cases that when the far-field applied loading is such that our "optimal" choice of the Cosserat parameter does not provide an exact match between the effective Cosserat material's energy and that of the actual heterogeneous material, our optimal effective Cosserat material will still be an improvement over the standard effective Cauchy material for *all* equilibrium uniform plus linear far-field applied loadings (for compliant-inclusion-type composites).

The characteristic length divided by the radius of the inclusion multiplied now by the volume fraction to the power $-1/6$, i.e., $f^{-1/6}\ell/a$, is plotted in Fig. 5 versus the contrast in the inclusion/matrix shear moduli, μ_i/μ_m, so that a null contrast corresponds to a void, Eq. (33). The different curves in the figures refer to different values of Poisson ratios, the same investigated for plane strain (ν_m and ν_i each having values 0.49 and 0). The values of the curves at $\mu_i/\mu_m=0$ depend only on ν_m.

The figures show that the qualitative behavior is the same for the two-dimensional and three-dimensional cases: for a sufficiently compliant inclusion, a positive characteristic length for an effective Cosserat material is always found, which decreases to zero at sufficiently high inclusion stiffness. However, there are also important differences between the 2D and the 3D cases:

1. For all values of the Poisson ratios of the matrix and inclusion, Ξ_Θ vanishes when $\mu_i=\mu_m$ and then becomes negative for $\mu_i>\mu_m$. Therefore, due to the effect of the torsion mode and in contrast to the 2D case, it is always impossible to produce a positive characteristic length ℓ for $\mu_i>\mu_m$, regardless of the values of the Poisson ratios, so that $\ell=0$ always results for $\mu_i \geqslant \mu_m$ (and not only for the special case $\nu_m=\nu_i$);
2. The curve for ℓ for the case $\nu_i=0$ and $\nu_m=0.49$ for 3D displays a jump to zero (not found for 2D deformations) at $\mu_i=\mu_m$. This behavior, occurring when $\nu_m>\nu_i$, is related to torsion and to the fact that η simultaneously tends to the limit -1. This means that the quantity $\ell^2(1+\eta)$, related to the characteristic length in torsion, is not discontinuous and correctly approaches zero when μ_i/μ_m tends to 1; and
3. *Result* 3. The characteristic length is substantially smaller in three dimensions than in two. This is partially due to the fact that $\ell \propto af^{1/6}$ in three dimensions, whereas $\ell \propto a$ in two dimensions. The figures show that the largest characteristic length (strongest Cosserat effect) occurs for an incompressible matrix containing voids ($\nu_m=0.5$, $\mu_i=0$), in which case

$$\ell \approx 0.702af^{1/6}, \quad \ell = \frac{\sqrt{\pi}}{2}a \approx 0.886a \tag{35}$$

for 3D and 2D, respectively. For example, if $f=0.1$, Eqs. (35) show ℓ/a in 3D to be 54% of that in 2D.

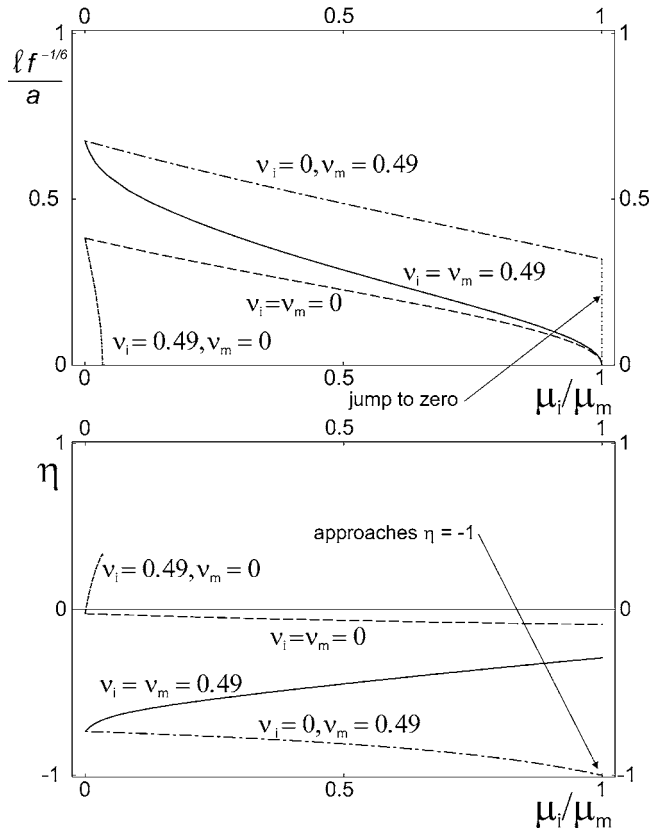

Fig. 5 Characteristic length divided by spherical inclusion radius and multiplied by $f^{-1/6}$ (top) and parameter η (bottom) for a homogeneous Cosserat material deduced from homogenization of a matrix containing a dilute distribution of spherical inclusions (Eq. (31))

6 Unconstrained Cosserat Materials do not Change Results 1, 2, and 3

At this point we are in a position to address the following question: can Result 1, stating that Cosserat effects only arise for inclusions less stiff than the matrix, be changed by making recourse to a more general theory of micropolar behavior than the constrained-rotation theory of Eq. (11)? Moreover, does Result 2, providing a closed-form formula for the characteristic length ℓ, and consequent Result 3, change if a general theory of micropolar behavior is assumed? The answers to these questions turn out to be negative, but they require a digression.

A general isotropic, linear micropolar material is characterized by the following constitutive equations [16,2]

$$\Sigma_{ij} = \lambda \varepsilon_{kk} \delta_{ij} + 2\mu \varepsilon_{ij} + \gamma e_{ijk}(\omega_k - \phi_k),$$

$$\mu_{ij} = \alpha \phi_{k,k} \delta_{ij} + 4\mu \ell^2 (\phi_{j,i} + \eta \phi_{i,j}) \tag{36}$$

where Σ_{ij} and μ_{ij} are the asymmetric force-stress and couple-stress tensors, respectively, and ω_k and ϕ_i are the macro- and micro-axial rotation vectors, respectively. Constants λ and μ play the role of the usual Lamé moduli of Cauchy elasticity, and α, η, γ, and ℓ are new material constants.

The important point is to note that Eqs. (11) are obtained from Eqs. (36) by taking $\phi_k = \omega_k$; then Σ_{ij} and μ_{ij} reduce to σ_{ij} (the symmetric part of the stress tensor) and m_{ij} (the deviator of the couple-stress tensor), respectively, and the terms containing α and γ in Eqs. (36) become identically zero.

Now we note that in the unconstrained theory, kinematical boundary conditions must involve prescription of displacements, macrorotations, and microrotations. If we make the sensible choice that the microrotations are identical to the macrorotations *on the boundary* and these are those arising from displacements Eqs. (6), then a (unique) solution to the full unconstrained theory produces the same energy Eq. (14). The same results for ℓ, Eqs. (22) and (31), are obtained. Now, however, parameters α and γ remain undetermined. Thus we find no advantage to use of the more complex unconstrained Cosserat model in the homogenization problem, and indeed we find the constrained-rotation model employed by Koiter [15] to have the great advantages of simplicity and physical transparency.

7 Experiments and Applications

We have already reported that our results explain and confirm the Gauthier [7] experimentally based claim that "an anti-micropolar phenomenon" is found for inclusions stiffer than the matrix. For inclusions less stiff than the matrix, our theory provides Cosserat parameters ℓ and η (only ℓ for plane strain) for the effective material which exactly match two quadratic deformation modes (one in plane strain), so that these parameters would be found in an ideal experiment performed on a specimen, when the boundary conditions corresponding to those modes are imposed. With the exception of an incompressible matrix material, the quadratic modes correspond to a combination of bending, torsion, and other modes, which are usually not experimentally investigated.

7.1 Bending and Torsion Experiments, and Applications Involving Pure Bending and Torsion Loading. Common experiments involve bending (usually bending of a plate deformed in plane strain) and torsion (usually of a bar with circular cross section). Performing such experiments will not in general (again, with the exception of plane-strain bending of a composite with an incompressible matrix material) yield our Cosserat parameters. This is because we have selected these to give the greatest possible improvement over the effective Cauchy material for all possible imposed linear plus quadratic displacement fields, such that the effective Cosserat material is never stiffer than the actual heterogeneous one. If, however, the applied loading of interest is known to consist of uniform plus pure bending loading in 2D, or uniform plus pure bending and pure torsion loading in 3D, the effective Cosserat parameters can be chosen to produce an exact energy match between the effective Cosserat material and the actual heterogeneous one.

In particular, for plane-strain deformations of a slab containing a dilute distribution of *cylindrical inclusions* (with axis parallel to the depth)

$$\ell_{\text{2D-bending}} = a\sqrt{\frac{\pi \Xi_R}{2}} \tag{37}$$

with Ξ_R given by Eq. $(8)_1$, provides an exact match for a plane strain bending experiment.

For plane-strain deformations of a slab containing a dilute distribution of *spherical inclusions* (note that, due to the plane strain constraint, parameter η does not enter)

$$\ell_{\text{3D plane-strain bending}} = a f^{1/6}\left(\frac{4\pi}{3}\right)^{1/3}\sqrt{\frac{\Xi_R}{2}} \tag{38}$$

where Ξ_R is given by Eq. $(10)_1$, gives an exact match for a plane-strain bending experiment.

For torsion of a cylindrical specimen (of circular cross section) containing a dilute distribution of *spherical inclusions*

$$(\ell\sqrt{1+\eta})_{\text{torsion cylindrical bar}} = af^{1/6}\left(\frac{4\pi}{3}\right)^{1/3}\sqrt{\frac{\Xi_\Theta}{3}} \qquad (39)$$

where Ξ_Θ is given by Eq. $(10)_3$, gives an exact match. Obviously, ℓ and η can be chosen to satisfy Eqs. (38) and (39) simultaneously.

7.2 A Comparison With Existing Experimental Results. It is interesting now to compare our results with experiments performed on material containing compliant inclusions, for instance voids. In particular, our results indicate that the most effective experimental setting to display Cosserat effects would be a material containing cylindrical voids deformed in plane strain, with a matrix Poisson's ratio tending to the limit value 0.5; for instance, a rubber block with cylindrical holes. Unfortunately, nothing like this experimental setup is available in the literature and also nothing pertaining to *dilute* suspensions of *spherical voids*.

The only results that we were able to find are those by Lakes [2] pertaining to two foams with nearly spherical voids. Specifically, one material is a syntactic foam consisting of hollow glass microbubbles embedded in an epoxy matrix, for which the mean diameter of voids is 0.125 mm and the volume fraction is 0.468. The second material is a high-density rigid polyurethane closed-cell foam, for which the mean diameter of voids is 0.1 mm and the volume fraction is 0.690. Within the general Cosserat framework Eqs. (36), Lakes [2] finds $\ell=0.032$ mm for the first material and $\ell=0.327$ mm for the second. Lakes also determines the quantity $\ell\sqrt{2(1+\eta)}$, which he estimates to be 0.065 mm and 0.62 mm, respectively.

There are several difficulties in attempting to compare our results with these materials:

1. The void volume fraction is so high that the dilute approximation is almost certainly not directly applicable;
2. The mechanical properties of the matrix material are not available;[2] and
3. The voids in the first material are coated by a glass shell of unknown stiffness.

Since these factors make a precise comparison impossible, we simply employ our model results with $\nu_m=1/2$, Eqs. (34), to make an order-of-magnitude comparison. Thus Eqs. (34) give $\ell=0.039$ mm and $\ell\sqrt{2(1+\eta)}=0.030$ mm for the first material and $\ell=0.033$ mm and $\ell\sqrt{2(1+\eta)}=0.025$ mm for the second. These results are only in qualitative agreement with the experimental findings; however, they are consistent with the fact that our model, based on the dilute approximation, underestimates the characteristic length ℓ for the given high values of the pore volume fractions. The fact that the characteristic length is better predicted for the first material than for the second is probably a consequence of the presence of the glass shell coating the voids, providing a stiffness, which strongly decreases ℓ.

8 Summary of General Methodology

Here we summarize the general methodology proposed in this paper and employed in the specific cases of a matrix containing a dilute suspension of spherical or circular cylindrical inclusions. We emphasize that our general methodology is not restricted to composites consisting of a matrix containing a dilute concentration of another phase. To determine the effective moduli for a homogeneous Cosserat-elastic material that best approximates a heterogeneous Cauchy-elastic material under general applied loadings, one first determines the effective Cauchy-elastic moduli in the standard manner (i.e., using the most accurate approach available from standard composite materials theory. We emphasize that we regard the uniform loading as the primitive case, so that this initial determination will not be affected by subsequent calculations). One then needs to compute the elastic energy in the heterogeneous material of interest when this is subjected to a general equilibrium linearly varying applied traction (or quadratically varying displacements) on the boundary. One then compares this energy to the energy computed for the homogeneous Cosserat material (whose Cauchy moduli have already been determined via the standard homogenization approach) subjected to the same quadratically varying displacements and rotations as in the Cauchy solution, and one chooses the Cosserat parameters so that these two energies are in closest possible agreement. In the specific cases analyzed in this paper, the Cosserat length is nonzero when the heterogeneous material is less stiff than its predominant phase, and zero otherwise.

9 Conclusions

It has been shown that a dilute dispersion of elastic isotropic spherical inclusions in a 3D composite (and infinitely long, parallel circular cylindrical inclusions in a 2D one) produce Cosserat effects when the inclusions are less stiff than the matrix. The effects induce a characteristic length in three dimensions

$$\ell \propto af^{1/6}$$

and one in two dimensions

$$\ell \propto a$$

where a is the inclusion radius and f the volume fraction of the inclusion material. The maximum characteristic length occurs when the inclusions are cavities, and the matrix material is incompressible; this length is substantially larger in 2D versus 3D for cavities having the same radius. Cosserat effects are on the other hand excluded for the opposite situation of inclusions having stiffnesses equal to or greater than that of the matrix.

An important practical implication of our findings is that the response of a composite material containing inclusions less stiff than the matrix and subjected to nonuniform stressing can be more accurately represented by a homogeneous Cosserat material with appropriately chosen moduli than by a standard (Cauchy) effective material.

Acknowledgment

We thank Professor R. S. Lakes (University of Wisconsin-Madison) for helpful discussions. D.B. acknowledges financial support from MURST-Cofin 2005 (Prot. No. 2005085973–002). W.J.D. thanks Dr. W. G. Wolfer for his interest in this work and for support from Lawrence Livermore National Laboratory under Contract W-7405-ENG-48 with the U.S. Department of Energy. W.J.D. also acknowledges support from the Italian Ministry Research Grant "Rientro dei cervelli" MIUR Grant No. 26/1/2001.

Appendix A: The State of the Art on Cosserat Effects as Deduced From Elastic, Inhomogeneous Media

The literature on Cosserat effects arising from heterogeneous media is rife with conflicting views. Berglund [17], claiming that previous results [18–20] were inconsistent, provides two theoretical arguments to *disprove micropolar effects*, employing both a discrete structural model of a cubic lattice and a framework for homogenization of a heterogeneous continuum. These appear to be far from conclusive, since the former invokes reduction of structural dimensions to zero (which is inconsistent with the fact that Cosserat effects should be related to some non-null characteristic microstructural length) and the latter does indeed predict some micropolar effects, which are then argued to be negligible. On the contrary, Cosserat behavior was found by Wang and Stronge [21] for a hexagonal lattice. Moreover, certain theoretical arguments *in favor* of Cosserat behavior have been provided by Achenbach and Hermann [22] and Beran and McCoy [23], but the

[2]Only ν_m is needed to determine ℓ. However, the knowledge of μ_m would allow us to determine $\bar{\mu}$ and $\bar{\kappa}$ from Eqs. (1), which compared to experimental results by Lakes would permit an assessment of the quality of the estimate.

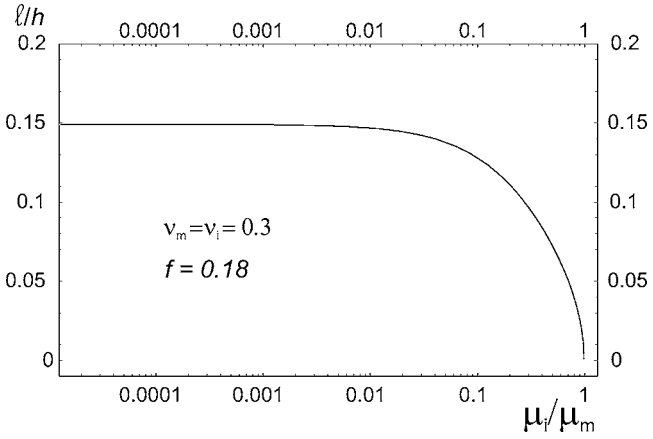

Fig. 6 Characteristic length divided by the cell size for volume fraction of disperse phase $f=0.18$, for a Cosserat material deduced from homogeneization of a matrix containing a dilute distribution of parallel, infinite circular cylindrical inclusions (plane strain, Eq. (21))

former holding only in certain circumstances involving dynamical effects and the latter apparently finally disproving the effects for composites with homogeneous and isotropic statistics of inclusions. Recently, Forest [24], Ostoja-Starzewski et al. [25], and Bouyge et al. [26] provided numerical finite element investigations supporting Cosserat effects in heterogeneous materials. Forest treats an anisotropic composite with an unusual microstructure, and does not directly provide values for the Cosserat characteristic length. The latter two papers treat plane problems of a matrix containing a dispersion of circular inclusions; they find a nonzero Cosserat length both for inclusions stiffer and more compliant than the matrix, a fact contradicted previously by experiments [6,7], and now by the analytical results derived in the present paper.

When Eq. (21) is plotted using a semi-logarithmic scale, such as that employed in Ref. [26] for their parameter values of $\nu_i=\nu_m=0.3$ and $f=0.18$, we obtain the graph shown in Fig. 6. The numerical values at high contrast are similar to those found in Ref. [26] (their Fig. 8), but our results: (1) correctly approach zero when the elastic mismatch disappears (while a nonzero characteristic length is found in Ref. [25] even for zero mismatch); and (2) show that Cosserat effects are excluded for mismatch greater than 1 (in which case ℓ would be imaginary).

Appendix B: Plane-Strain Solution of an Elastic Circular Inclusion in an Infinite Elastic Matrix, Subject to Remote Displacements Field Eqs. (5)

We use the Kolosov–Muskhelishvili [11] complex potentials representation of the general solution for plane problems in homogeneous isotropic linear elastostatics, which in polar coordinates is

$$u_r + \mathrm{i}u_\vartheta = \frac{1}{2\mu}\mathrm{e}^{-\mathrm{i}\vartheta}[\kappa\varphi(z) - z\overline{\varphi'(z)} - \overline{\psi(z)}] \tag{B1}$$

$$\sigma_{rr} + \sigma_{\vartheta\vartheta} = 4\,\mathrm{Re}[\varphi'(z)]$$

$$\sigma_{\vartheta\vartheta} - \sigma_{rr} + 2i\sigma_{r\vartheta} = 2e^{2i\vartheta}[\bar{z}\varphi''(z) + \psi'(z)] \tag{B2}$$

where $z=x_1+ix_2=re^{i\vartheta}$, $\varphi(z)$ and $\psi(z)$ are analytic functions, Re[] denotes the real part, and $\kappa=3-4\nu$ for plane strain.

First, we consider a pure bending far-field applied loading, corresponding to

$$\sigma_{22} = mx_1, \quad \sigma_{11} = \sigma_{12} = 0 \quad \text{for } r \to \infty \tag{B3}$$

or, in terms of complex potentials

$$\varphi(z) = \psi(z) = \frac{m}{8}z^2, \quad \text{for } |z| \to \infty \tag{B4}$$

The solution for a matrix containing an inclusion of radius a is

$$\varphi(z) = \frac{m}{8}z^2 + \frac{\mu_i - \mu_m}{2(\kappa_m\mu_i + \mu_m)}\frac{ma^4}{4z^2} \tag{B5}$$

$$\psi(z) = \frac{m}{8}z^2 + \frac{\kappa_m\mu_i - \mu_m\kappa_i}{\mu_i + \kappa_i\mu_m}\frac{ma^4}{8z^2} + \frac{\mu_i - \mu_m}{\kappa_m\mu_i + \mu_m}\frac{ma^6}{4z^4} \tag{B6}$$

in material outside the inclusion, and

$$\varphi(z) = \frac{(\kappa_m+1)\mu_i}{\mu_i + \kappa_i\mu_m}\frac{m}{8}z^2 - \frac{\mu_i}{\mu_m}\frac{\mu_i + \mu_m(\kappa_i - \kappa_m - 1)}{\kappa_i(\mu_i + \kappa_i\mu_m)}\frac{ma^2}{4} \tag{B7}$$

$$\psi(z) = \frac{(\kappa_m+1)\mu_i}{\kappa_m\mu_i + \mu_m}\frac{m}{8}z^2 \tag{B8}$$

in material inside the inclusion.

Second, we consider a quadratic far-field applied displacement field, corresponding to

$$u_1 = \tilde{\beta}_{13}\left(x_1^2 - \frac{\kappa_m+1}{\kappa_m-1}x_2^2\right), \quad u_2 = u_3 = 0 \quad \text{for } r \to \infty \tag{B9}$$

or, in terms of complex potentials

$$\varphi(z) = \frac{\mu_m\tilde{\beta}_{13}}{\kappa_m-1}z^2, \quad \psi(z) = -\frac{\mu_m\kappa_m\tilde{\beta}_{13}}{\kappa_m-1}z^2 \quad \text{for } |z| \to \infty \tag{B10}$$

The solution is

$$\varphi(z) = \frac{\mu_m\tilde{\beta}_{13}}{\kappa_m-1}z^2 + \frac{\mu_m - \mu_i}{\kappa_m\mu_i + \mu_m}\frac{a^4\mu_m\kappa_m\tilde{\beta}_{13}}{z^2(\kappa_m-1)} \tag{B11}$$

$$\psi(z) = -\frac{\mu_m\kappa_m\tilde{\beta}_{13}}{\kappa_m-1}z^2 + \frac{\kappa_m\mu_i - \mu_m\kappa_i}{\mu_i + \kappa_i\mu_m}\frac{a^4\mu_m\tilde{\beta}_{13}}{z^2(\kappa_m-1)} + \frac{\mu_m - \mu_i}{\kappa_m\mu_i + \mu_m}\frac{2a^6\mu_m\kappa_m\tilde{\beta}_{13}}{z^4(\kappa_m-1)} \tag{B12}$$

in material outside the inclusion, and

$$\varphi(z) = \frac{(\kappa_m+1)\mu_i}{\mu_i + \kappa_i\mu_m}\frac{\mu_m\tilde{\beta}_{13}}{\kappa_m-1}z^2 - \frac{\mu_i}{\mu_m}\frac{\mu_i + \mu_m(\kappa_i - \kappa_m - 1)}{\kappa_i(\mu_i + \kappa_i\mu_m)}\frac{2a^2\mu_m\tilde{\beta}_{13}}{\kappa_m-1} \tag{B13}$$

$$\psi(z) = -\frac{(\kappa_m+1)\mu_i}{\kappa_m\mu_i + \mu_m}\frac{\mu_m\kappa_m\tilde{\beta}_{13}}{\kappa_m-1}z^2 \tag{B14}$$

in material inside the inclusion.

Appendix C: Three-Dimensional Solution of a Spherical Elastic Inclusion in an Infinite Elastic Matrix, Subject to Remote Displacements Field Eqs. (6)

C.1 Torsion Prescribed at Infinity

First, we consider an applied far-field torsion, consisting of a different (in general) angle of twist/length applied about each of the three Cartesian axes. This corresponds to the equilibrium displacement field

$$u_1 = (\Theta_2 - \Theta_3)x_2x_3, \quad u_2 = (\Theta_3 - \Theta_1)x_3x_1,$$

$$u_3 = (\Theta_1 - \Theta_2)x_1x_2 \quad \text{for } r \to \infty \tag{C1}$$

or, in spherical coordinates

$$u_r = 0, \quad u_\vartheta = -(\Theta_1 - \Theta_2)r^2\sin\phi\cos\phi\sin\vartheta$$

$$u_\phi = -\frac{\Theta_1+\Theta_2-2\Theta_3+(\Theta_1-\Theta_2)\cos 2\phi}{4} r^2 \sin 2\vartheta \quad \text{for } r\to\infty \tag{C2}$$

The solution to this applied far-field, satisfying equilibrium everywhere, and displacement and traction continuity across the inclusion-matrix boundary $r=a$, is

$$u_r = 0$$

$$u_\vartheta = -(\Theta_1-\Theta_2)\sin\phi\cos\phi\sin\vartheta\left[r^2+\frac{a^5(\mu_m-\mu_i)}{r^3(4\mu_m+\mu_i)}\right]$$

$$u_\phi = -\frac{\Theta_1+\Theta_2-2\Theta_3+(\Theta_1-\Theta_2)\cos 2\phi}{4}\sin 2\vartheta\left[r^2+\frac{a^5(\mu_m-\mu_i)}{r^3(4\mu_m+\mu_i)}\right] \tag{C3}$$

in material outside the inclusion, and

$$u_r = 0$$

$$u_\vartheta = -5\mu_m r^2\frac{\Theta_1-\Theta_2}{4\mu_m+\mu_i}\sin\phi\cos\phi\sin\vartheta$$

$$u_\phi = -5\mu_m r^2\frac{\Theta_1+\Theta_2-2\Theta_3+(\Theta_1-\Theta_2)\cos 2\phi}{4(4\mu_m+\mu_i)}\sin 2\vartheta \tag{C4}$$

in material inside the inclusion.

C.2 Bending and the Other Equilibrium Quadratic Displacement Modes Prescribed at Infinity

Second, we consider the applied far-field equilibrium displacement field

$$u_1 = -\frac{1}{2R_{23}}\left(x_2^2+\frac{\nu_m}{1-\nu_m}x_1^2\right)-\frac{1}{2R_{32}}\left(x_3^2+\frac{\nu_m}{1-\nu_m}x_1^2\right)+(\tilde\beta_{13}+\tilde\beta_{12})x_1^2-2\frac{1-\nu_m}{1-2\nu_m}(\tilde\beta_{13}x_2^2+\tilde\beta_{12}x_3^2)$$

$$u_2 = \frac{x_2x_1}{R_{23}}, \quad u_3 = \frac{x_3x_1}{R_{32}} \quad \text{for } r\to\infty \tag{C5}$$

from which the general representation Eq. (6) can be obtained by using superposition and adding torsion. The bending we treat is plane-strain bending, while Sen [13] and Das [14] have considered a pure (uniaxial-stress) bending. Their case is recovered by redefining coefficients $1/R_{23}$ and $1/R_{32}$ as follows

$$\frac{1}{R_{23}} = -\frac{\nu_m A}{E_m}+\frac{C}{E_m} \quad \text{and} \quad \frac{1}{R_{32}} = \frac{A}{E_m}-\frac{\nu_m C}{E_m} \tag{C6}$$

where A and C are arbitrary constants and E_m is the elastic modulus of the matrix material. The case $C=0$ is that analyzed in Refs. [13,14], and this is sufficient to solve the general case Eq. (C6) via superposition. We note also that the modes defined by coefficients $\tilde\beta_{ij}$ can be redefined in a way similar to Eq. (C6), and again by superposition it is sufficient to solve for the case

$$\tilde\beta_{13} = -\frac{1-2\nu}{3-4\nu}\tilde\beta_{12} \tag{C7}$$

In polar coordinates, the far-field representation Eq. (C5) with Eq. (C6) (taking $C=0$ and all other coefficients null) has the same structure as Eq. (C5) with Eq. (C7) (with all other coefficients null). This is

$$u_r = Br^2\cos\phi\sin\vartheta(c_1+c_2\cos 2\vartheta)$$

$$u_\vartheta = Br^2\cos\phi\cos\vartheta(c_3+c_2\cos 2\vartheta)$$

$$u_\phi = Br^2\sin\phi(c_4+c_5\cos 2\vartheta) \tag{C8}$$

where

$$B = \frac{A}{4E_m}, \quad c_1 = c_4 = c_3+4 = 1-\nu_m, \quad c_2 = c_5 = 1+\nu_m \tag{C9}$$

for bending, while

$$B = -\frac{2(1-\nu_m)\tilde\beta_{12}}{(1-2\nu_m)(3-4\nu_m)}, \quad c_1 = c_3 = -c_4 = 1-\nu_m,$$

$$c_2 = -c_5 = 2-3\nu_m \tag{C10}$$

for the mode defined by coefficients $\tilde\beta_{ij}$.

The solution to this applied far-field displacement field that satisfies equilibrium everywhere, and displacement and traction continuity across the inclusion-matrix boundary $r=a$, is

$$u_r = B\cos\phi\sin\vartheta\left[r^2(c_1+c_2\cos 2\vartheta)+\frac{a^5(k_1+k_2\cos 2\vartheta)}{r^3}+\frac{a^7(k_3+k_4\cos 2\vartheta)}{r^5}\right]$$

$$u_\vartheta = B\cos\phi\cos\vartheta\left[r^2(c_3+c_2\cos 2\vartheta)+\frac{a^5(k_5+k_6\cos 2\vartheta)}{r^3}+\frac{a^7(k_7+k_8\cos 2\vartheta)}{r^5}\right]$$

$$u_\phi = B\sin\phi\left[r^2(c_4+c_5\cos 2\vartheta)+\frac{a^5(k_9+k_{10}\cos 2\vartheta)}{r^3}+\frac{a^7(k_{11}+k_{12}\cos 2\vartheta)}{r^5}\right] \tag{C11}$$

in material outside the inclusion, and

$$u_r = Br^2\cos\phi\sin\vartheta\left(\frac{c_0}{r^2}+m_1+m_2\cos 2\vartheta\right)$$

$$u_\vartheta = Br^2\cos\phi\cos\vartheta\left(\frac{c_0}{r^2}+m_3+m_2\cos 2\vartheta\right)$$

$$u_\phi = Br^2\sin\phi\left(-\frac{c_0}{r^2}+m_4+m_5\cos 2\vartheta\right) \tag{C12}$$

in material inside the inclusion. (The Sen [14] solution violates displacement continuity across $r=a$ since it is missing the c_0 terms in Eq. (C12).) All coefficients appearing in the above Eqs. (C11) and (C12) are dimensionless and are defined as

$$k_1 = \frac{12k_8(1-4\nu_m)-5[4c_1(2-3\nu_m)-3c_2-3m_1(1-4\nu_m)]}{15(1-4\nu_m)}-\frac{15c_2-25m_1+k_8(22-28\nu_m)}{15(1-4\nu_i)}$$

$$k_2 = \frac{14k_8(3-2\nu_m)}{15}, \quad k_3 = -\frac{4k_8}{5}, \quad k_4 = -\frac{4k_8}{3},$$

$$k_5 = -\frac{k_1}{2}-k_{10}+\frac{k_2(1+2\nu_m)}{2(3-2\nu_m)}$$

$$k_6 = k_2-\frac{5k_2}{2(3-2\nu_m)}, \quad k_7 = -\frac{7k_8}{15}$$

$$k_8 = \frac{15c_2[E_m(1+\nu_i) - E_i(1+\nu_m)]}{2E_i(1+\nu_m)(11-14\nu_m) + E_m(13-7\nu_m)(1+\nu_i)}$$

$$k_9 = \frac{k_1}{2} - \frac{k_2(1-\nu_m)}{3-2\nu_m}$$

$$k_{10} = \frac{E_m(1+\nu_i) - E_i(1+\nu_m)}{E_i(1+\nu_m) + 4E_m(1+\nu_i)} \left\{ \frac{2\nu_m(c_1+3c_2+2c_3) - 3c_1 - c_3}{1-4\nu_m} + \frac{c_2[E_i(27-\nu_m-28\nu_m^2) + 4E_m(2+7\nu_m)(1+\nu_i)]}{2E_i(1+\nu_m)(11-14\nu_m) + E_m(1+\nu_i)(13-7\nu_m)} \right\}$$

$$k_{11} = -\frac{k_8}{5}, \quad k_{12} = -\frac{k_8}{3}$$

$$c_0 = \frac{-5(5c_1-3c_2)}{15(1-4\nu_m)} - \frac{5(3c_2-5m_1) + k_8(22-28\nu_m)}{15(1-4\nu_i)}$$

$$m_1 = \frac{5(1-\nu_m)[26c_1-3c_2-14(c_1+3c_2)\nu_m]}{3(1-4\nu_m)(13-7\nu_m)} - \frac{(5c_1-3c_2)(1-\nu_m)[5E_m+2E_i(1+\nu_m)]}{3(1-4\nu_m)[2E_m(2-3\nu_i)+E_i(1+\nu_m)]} - \frac{42c_2E_i(1-\nu_m)(1+\nu_m)(11-14\nu_m)}{(13-7\nu_m)[2E_i(1+\nu_m)(11-14\nu_m)+E_m(1+\nu_i)(13-7\nu_m)]}$$

$$m_2 = c_2 + \frac{2k_8(11-14\nu_m)}{15}$$

$$m_3 = -k_{10} + \frac{1}{2}\left(c_1 + 2c_3 + \frac{5c_1-3c_2}{1-4\nu_m} + \frac{3c_2}{1-4\nu_i}\right) - \frac{m_1(3-2\nu_i)}{1-4\nu_i} + \frac{k_8[27+24\nu_i-28\nu_m(1+2\nu_i)]}{15(1-4\nu_i)}$$

$$m_4 = \frac{m_1(3-2\nu_i) - 2m_2(1-\nu_i)}{1-4\nu_i},$$

$$m_5 = -m_3 + \frac{m_2(1+2\nu_i) - m_1(3-2\nu_i)}{1-4\nu_i}$$

where E_m, E_i, and ν_m, ν_i are the elastic moduli and Poisson's ratios of the matrix and inclusion materials, respectively.

References

[1] Lakes, R. S., 1983, "Size Effects and Micromechanics of a Porous Solid," J. Mater. Sci., **18**, pp. 2572–2581.

[2] Lakes, R. S., 1986, "Experimental Microelasticity of Two Porous Solids," Int. J. Solids Struct., **22**, pp. 55–63.

[3] Lakes, R. S., 1995, "Experimental Methods for Study of Cosserat Elastic Solids and Other Generalized Continua," *Continuum Models for Materials with Micro-Structure*, H. B. Muhlhaus, ed., Wiley, New York, pp. 1–22.

[4] Yang, J. F. C., and Lakes, R. S., 1981, "Transient Study of Couple Stress in Compact Bone: Torsion," J. Biomech. Eng., **103**, pp. 275–279.

[5] Yang, J. F. C., and Lakes, R. S., 1982, "Experimental Study of Micropolar and Couple Stress Elasticity in Bone in Bending," J. Biomech., **15**, pp. 91–98.

[6] Gauthier, R. D., and Jahsman, W. E., 1975, "A Quest for Micropolar Elastic Constants," ASME J. Appl. Mech., **42**, pp. 369–374.

[7] Gauthier, R. D., 1982, "Experimental Investigation on Micropolar Media," *Mechanics of Micropolar Media*, O. Brulin and R. K. T. Hsieh, eds., CISM Lecture Notes, World Scientific, Singapore, pp. 395–463.

[8] Eshelby, J. D., 1957, "The Determination of the Elastic Field of an Ellipsoidal Inclusion and Related Problems," Proc. R. Soc. London, Ser. A, **241**, pp. 376–396.

[9] Hashin, Z., 1959, "The Moduli of an Elastic Solid Containing Spherical Particles of Another Elastic Material," *Non-Homogeneity in Elasticity and Plasticity*, W. Olszak, ed., Pergamon, New York, pp. 463–478.

[10] Hashin, Z., and Rosen, W. B., 1964, "The Elastic Moduli of Fiber-Reinforced Materials," J. Appl. Mech., **31**, pp. 223–232.

[11] Muskhelishvili, N. I., 1953, *Some Basic Problems of the Mathematical Theory of Elasticity*, Noordhoff, Groningen, Holland.

[12] Sendeckyj, G. P., 1970, "Elastic Inclusion Problems in Plane Elastostatics," Int. J. Solids Struct., **6**, pp. 1535–1543.

[13] Sen, B., 1933, "On the Concentration of Stresses Due to a Small Spherical Cavity in a Uniform Beam Bent by Terminal Couples," Bull. Calcutta Math. Soc., **25**, pp. 107–114.

[14] Das, S. C., 1953, "On the Stresses Due to a Small Spherical Inclusion in a Uniform Beam Under Constant Bending Moment," Bull. Calcutta Math. Soc., **45**, pp. 55–63.

[15] Koiter, W. T., 1964, "Couple-Stresses in the Theory of Elasticity, Parts I and II," Proc. K. Ned. Akad. Wet., Ser. B: Phys. Sci., **67**, pp. 17–44.

[16] Nowacki, W., 1986, *Theory of Asymmetric Elasticity*, Pergamon, Oxford.

[17] Berglund, K., 1982, "Structural Models of Micropolar Media," *Mechanics of Micropolar Media (CISM Lecture Notes)*, O. Brulin and R. K. T. Hsieh, eds., World Scientific, Singapore, pp. 35–86.

[18] Dean, D. L., and Urgate, C. P., 1968, "Field Solutions for Two-Dimensional Frameworks" Int. J. Mech. Sci., **10**, pp. 315–339.

[19] Bažant, Z. P., and Christensen, M., 1972, "Analogy Between Micropolar Continuum and Grid Frameworks Under Initial Stress," Int. J. Solids Struct., **8**, pp. 327–346.

[20] Banks, C. B., and Sokolowski, U., 1968, "On Certain Two-Dimensional Applications of Couple-Stress Theory," Int. J. Solids Struct., **4**, pp. 15–29.

[21] Wang, X. L., and Stronge, W. J., 1999, "Micropolar Theory for Two-Dimensional Stresses in Elastic Honeycomb," Proc. R. Soc. London, Ser. A, **445**, pp. 2091–2116.

[22] Achenbach, J. D., and Herrmann, G., 1968, "Dispersion of Free Harmonic Waves in Fibre-Reinforced Composites," AIAA J., **6**, pp. 1832–1836.

[23] Beran, M. J., and McCoy, J. J., 1970, "Mean Field Variations in a Statistical Sample of Heterogeneous Linearly Elastic Solids," Int. J. Solids Struct., **6**, pp. 1035–1054.

[24] Forest, S., 1998, "Mechanics of Generalized Continua: Construction by Homogenization," J. Phys. IV, **8**, pp. 39–48.

[25] Ostoja-Starzewski, M., Boccara, S., and Jasiuk, I., 1999, "Couple-Stress Moduli and Characteristic Length of Composite Materials," Mech. Res. Commun., **26**, pp. 387–397.

[26] Bouyge, F., Jasiuk, I., and Ostoja-Starzewski, M., 2001, "A Micromechanically Based Couple-Stress Model of an Elastic Two-Phase Composite," Int. J. Solids Struct., **38**, pp. 1721–1735.